Acta Crystallographica Section F
**Structural Biology and Crystallization Communications**
ISSN 1744-3091

# Effect of leucine-to-methionine substitutions on the diffraction quality of histone chaperone SET/TAF-I$\beta$/INHAT crystals

**Miki Senda,[a] Shinsuke Muto,[b,c] Masami Horikoshi[b,c] and Toshiya Senda[d]***

[a]Structure Guided Drug Development Project, Research and Development Department, Japan Biological Informatics Consortium (JBIC), 2-42 Aomi, Koto-ku, Tokyo 135-0064, Japan, [b]Laboratory of Developmental Biology, Institute of Molecular and Cellular Biosciences, The University of Tokyo, 1-1-1 Yayoi, Bunkyo-ku, Tokyo 113-0032, Japan, [c]Horikoshi Gene Selector Project, Exploratory Research for Advanced Technology (ERATO), Japan Science and Technology Corporation (JST), 5-9-6 Tokodai, Tsukuba, Ibaraki 300-2635, Japan, and [d]Biomedicinal Information Research Center (BIRC), National Institute of Advanced Industrial Science and Technology (AIST), 2-42 Aomi, Koto-ku, Tokyo 135-0064, Japan

Correspondence e-mail: toshiya-senda@aist.go.jp

Received 1 May 2008
Accepted 8 September 2008



One of the most frequent problems in crystallization is poor quality of the crystals. In order to overcome this obstacle several methods have been utilized, including amino-acid substitutions of the target protein. Here, an example is presented of crystal-quality improvement by leucine-to-methionine substitutions. A variant protein with three amino-acid substitutions enabled improvement of the crystal quality of the histone chaperone SET/TAF-I$\beta$/INHAT when combined with optimization of the cryoconditions. This procedure improved the resolution of the SET/TAF-I$\beta$/INHAT crystals from around 5.5 to 2.3 Å without changing the crystallization conditions.

## 1. Introduction

To improve crystal quality for structure determination, variant proteins with amino-acid substitution(s) and/or deletion(s) of some residues have been utilized (Lawson *et al.*, 1991; McElroy *et al.*, 1992; Jenkins *et al.*, 1995; Longenecker *et al.*, 2001; Mateja *et al.*, 2002; Zhou *et al.*, 2003; Derewenda & Vekilov, 2006; Cooper *et al.*, 2007). Perturbations of the conformation and/or the stability of the variant proteins seem to affect the crystal quality. Crystallization of the target protein from different species, another well known 'trick' for improving protein crystals, can be regarded as a method that uses naturally occurring mutations.

The variant proteins that are useful for crystallization can be divided into two types. The first type involves the truncation of an unstructured or mobile region of the protein, such as an acidic tail, in order to change or improve the crystal packing (Chait, 1994). This method is one of the standard strategies in protein crystallography. The second type involves amino-acid substitution of the protein. When the crystal structure of the target protein is already known, inter-protein interactions in the crystal can be optimized through amino-acid substitution (McElroy *et al.*, 1992; Mateja *et al.*, 2002). The crystallization of proteins for which the structure is unknown can also be improved by amino-acid substitution (Zhou *et al.*, 2003).

Other examples have shown that amino-acid substitution can enable the crystallization of a protein for which the wild type could not be crystallized (Lawson *et al.*, 1991; Longenecker *et al.*, 2001; Schlatter *et al.*, 2005). The surface-entropy reduction method, which is the most intensively studied method involving amino-acid substitution in crystallization, has succeeded in crystallizing difficult proteins (Derewenda & Vekilov, 2006; Cooper *et al.*, 2007). It is of note that most known examples targeted exposed residues, with the expectation of changing the epitopes of inter-protein contacts and/or reducing the entropic effect.

The effect of amino-acid substitution(s) of buried hydrophobic residues on crystal quality, however, has not been well studied. In the present study, we planned to use the amino-acid substitution of leucine/isoleucine to methionine. The effects of this replacement on protein structure have been intensively studied using T4 lysozyme and hen egg-white lysozyme, showing that this replacement is un-

**Table 1**
Comparison of crystal quality.

Means and standard deviations are given when multiple data sets were collected.

| Variant/soaking solution† | Soaking temperature (K) | Mosaicity | Resolution‡ (Å) | Overall *B*§ (Å$^2$) | $\Delta B$¶ (Å$^2$) | Space group |
|---|---|---|---|---|---|---|
| Wild type/30% trehalose (1) | 277 | 0.31 | 3.9 | 61.8 | 135.4 | *C*2 |
| *A*/30% trehalose (4) | 293 | 0.28 ± 0.07 | 3.8 ± 0.4 | 82.5 ± 6.9 | 94.3 ± 26 | *C*2 |
| *B*/30% trehalose (1) | 293 | 0.47 | 3.25 | 98.0 | 91.2 | *C*2 |
| *E*/30% trehalose (5) | 293 | 0.28 ± 0.09 | 3.1 ± 0.3 | 72.4 ± 10.7 | 78.4 ± 32 | *C*2 |
| *DEF*/30% trehalose (8) | 293 | 0.28 ± 0.16 | 2.9 ± 0.2 | 54.1 ± 7.6 | 52.6 ± 13 | $P2_1$ |
| *DEF*/30% trehalose (7) | 277 | 0.20 ± 0.03 | 2.7 ± 0.1 | 41.4 ± 7.4 | 39.7 ± 6.8 | $P2_1$ |
| *BEG*/30% trehalose (3) | 293 | 0.48 ± 0.16 | 3.7 ± 0.4 | 89.8 ± 18.9 | 72.4 ± 11 | *C*2 |
| *CEF*/30% trehalose (1) | 293 | 0.48 | 5.7 | 74.5 | 117.8 | *C*2 |
| *DEF*/30% glucose (1) | 277 | 0.40 | 3.4 | 70.0 | 87.3 | *C*2 |
| *DEF* (without soaking) (1) | — | 0.81 | 4.2 | 72.3 | 130.4 | *C*2 |
| *DEF*/trehalose (1) (cocrystal) | — | 0.32 | 3.0 | 54.2 | 77.7 | *C*2 |

† Numbers in parentheses show the number of data sets used in preparing the table. ‡ The resolution limit was determined with $R_{\rm mrgd\text{-}\mathit{F}}$ value (Diederichs & Karplus, 1997) less than 0.25. § Overall *B* factors were calculated using the *XDS* program package. ¶ $\Delta B$ represents the largest differences among the three '*B* factors' calculated for the three principal directions of the data set using the diffraction anisotropy server (Strong *et al.*, 2006).

likely to destroy the protein structure (Gassner *et al.*, 1996; Ohmura *et al.*, 2001). Therefore, this replacement seems to have potential for use in crystallization experiments.

Here, we present an example of crystal-quality improvement for the histone chaperone SET/TAF-I$\beta$/INHAT (hereafter referred to as TAF-I$\beta$) through leucine-to-methionine substitutions. Crystals of TAF-I$\beta$, which originally diffracted X-rays to 5.5 Å resolution, were substantially improved by a combination of leucine-to-methionine substitutions and optimization of the cryoconditions, resulting in crystal structure determination of TAF-I$\beta$ to 2.3 Å resolution by the multiwavelength anomalous diffraction (MAD) method (Muto *et al.*, 2007).

## 2. Materials and methods

### 2.1. Preparation, purification and crystallization of TAF-I$\beta\Delta$C variants

TAF-I$\beta\Delta$C is composed of residues 1–255 of TAF-I$\beta$. The mutant genes for the TAF-I$\beta\Delta$C variants were generated by site-directed PCR mutagenesis. The His-tagged TAF-I$\beta\Delta$C variants were overexpressed and purified as described previously (Muto *et al.*, 2004). The wild type and the *DEF* variant were shown to be fully active. No biochemical assays were performed for the other variants. Crystallizations of the TAF-I$\beta\Delta$C variants were performed by the sitting-drop vapour-diffusion method with a minor modification of the reported conditions (Muto *et al.*, 2004). TAF-I$\beta\Delta$C variants concentrated to 35–80 mg ml$^{-1}$ (Supplementary Table 1[1]) were used for crystallization by the sitting-drop vapour-diffusion method. The reservoir solution consisted of 2.40–2.85 *M* ammonium sulfate, 0.10 *M* sodium citrate pH 5.35–5.50, 0.20 *M* potassium sodium tartrate and 30 m*M* magnesium chloride. Since the TAF-I$\beta\Delta$C crystals typically grew in thin plate shapes, the concentration of ammonium sulfate in the reservoir solution was optimized in the range 2.40–2.85 *M* in increments of 0.050 *M* to obtain large and thick crystals. For the cocrystallization of the *DEF* variant of TAF-I$\beta\Delta$C with trehalose (see below), reservoir solution containing 7.5%(*w*/*v*) trehalose was utilized. The concentration of ammonium sulfate was optimized in the range 2.75–2.85 *M* in increments of 0.050 *M*. It is of note that the pH value was also optimized for some variants from 5.35 to 5.50 in increments of 0.05 (Supplementary Table 1[1]).

[1] Supplementary material has been deposited in the IUCr electronic archive (Reference: GJ5046).

Drops were prepared by mixing 3.0 µl protein solution with an equal volume of reservoir solution and were equilibrated against a 500 µl volume of reservoir solution at 293 K in an incubator. The crystals typically grew in a week. The crystals used for X-ray data collection were selected from the largest and thickest obtained. The crystals of the various mutants grew within a narrow range of conditions: 35–80 mg ml$^{-1}$ protein concentration, 2.40–2.85 *M* ammonium sulfate pH 5.35–5.50 (Supplementary Table 1[1]). For each variant, differences in crystallization conditions did not seem to affect crystal quality.

### 2.2. Crystal soaking and cryoprotection

Screening of cryoprotectant reagents was performed using glucose, glycerol and trehalose. A wild-type crystal was soaked at room temperature in artificial mother liquor (2.75 *M* ammonium sulfate, 0.10 *M* sodium citrate pH 5.4, 0.20 *M* potassium/sodium tartrate, 30 m*M* magnesium chloride) containing 30%(*w*/*v*) glucose, 30%(*v*/*v*) glycerol or 30%(*v*/*v*) trehalose for 30–60 s, mounted on a cryoloop (Hampton Research) and flash-cooled in an $N_2$ flow at 100 K. Inspection of the crystals was performed using an R-AXIS IV$^{++}$ imaging-plate system (Rigaku) mounted on a rotating-anode X-ray generator (FR-D, Rigaku) operated at 50 kV and 60 mA. Crystal quality was assessed using a few frames of the diffraction pattern. The effect of crystal annealing (see below) was also tested. Cryoprotection with trehalose gave the best results when combined with crystal annealing (see §3.1).

For data collection, two types of post-crystallization treatments with cryoprotectant were performed in the present study: crystal soaking and cryoprotection. The soaking experiment was performed as follows. Artificial mother liquor containing 30%(*w*/*v*) trehalose was added to the sitting drop at a 1:1 volume ratio and stored in an incubator. Therefore, the final concentration of trehalose was 15%(*w*/*v*) in the soaking experiment. In optimizing the soaking conditions, the soaking temperature (277 and 293 K) and soaking time (from 3 min to one week) were adjusted (see below).

Cryoprotection was performed using artificial mother liquor containing 30%(*w*/*v*) trehalose (the cryoprotectant solution). The crystals were cryoprotected using the same method for data collection at 95 K, with the exception of the *DEF*-05 crystal (Supplementary Table 2[1]). In most cases, cryoprotection was performed after the soaking experiment. The crystal was transferred from a droplet in the sitting-drop setting to the cryoprotectant solution and kept there for

30–60 s. The cryoprotected crystal was mounted on a cryoloop (Hampton Research) and then flash-cooled in an $N_2$ flow at 95 K.

In some cases, crystal annealing was performed after flash-cooling as follows. The cryocooled crystal was removed from the cold $N_2$ gas stream, placed in the cryoprotectant solution for 1 min and then recooled in the $N_2$-gas stream.

### 2.3. Data collection

All diffraction data were collected using an ADSC Quantum CCD detector on beamlines BL-5A, BL-6A, BL-18B and NW12A of the Photon Factory, KEK (Tsukuba, Japan) and a MAR CCD detector on beamline BL41XU of SPring-8 (Harima, Japan), except for the WT-01 data (Supplementary Table 2). Most data were collected at 95 K (Supplementary Table 2). Only the wild-type and variant *DEF* crystals were probed at room temperature. All diffraction data were processed and scaled using the programs *XDS* and *XSCALE* (Kabsch, 1993), with the exception of the WT-01 data (Supplementary Table 2). The WT-01 data were processed and scaled using *d*TREK* (Pflugrath, 1999). When preparing the tables, the resolution limit was determined as an $R_{\rm mrgd\text{-}\mathit{F}}$ value (Diederichs & Karplus, 1997) less than approximately 0.25 (Table 1, Supplementary Table 2). This criterion will be used in the discussion of the present study. It is of note that higher resolution diffraction data, which show $R_{\rm mrgd\text{-}\mathit{F}}$ values greater than 0.25, were used for the structure determination and crystallographic refinement (Muto *et al.*, 2007). The anisotropy of the diffraction data was analyzed using the diffraction anisotropy server (http://www.doe-mbi.ucla.edu/~sawaya/anisoscale/; Strong *et al.*, 2006).

## 3. Results

### 3.1. Quality of the initially obtained TAF-I$\beta$ crystal

Since the C-terminal acidic region of TAF-I$\beta$ (residues 226–277) is likely to be an unstructured region, residues 226–277 of TAF-I$\beta$ were truncated (Muto *et al.*, 2007). The initially obtained crystal of TAF-I$\beta\Delta$C diffracted X-rays to no more than 5.5 Å resolution and decayed rapidly at room temperature. Diffraction data collected at 95 K without cryoprotection were also poor (Supplementary Fig. 1*a*). Cryoprotectant screening was therefore performed.

In the screening, trehalose, glucose and glycerol were examined as cryoprotectants (see §2.2). Crystals that were cryoprotected with glucose and glycerol solutions only diffracted X-rays to approximately 7 Å resolution. The best diffraction pattern was obtained from a crystal that had been annealed after cryoprotection with trehalose; the crystal diffracted X-rays to approximately 4 Å resolution. Furthermore, soaking the crystal in trehalose solution [final concentration of 15%(*w*/*v*)] at 277 K for 20 h before cryoprotection and crystal annealing lead to a moderate improvement in diffraction quality, resulting in data collection at 3.9 Å resolution using synchrotron radiation (Table 1, Supplementary Fig. 1*b* and Supplementary Table 2). However, there were numerous streaky spots in the diffraction pattern. In addition, the diffraction patterns showed a highly anisotropic character (see the $\Delta B$ column of Table 1). Although the crystal diffracted X-rays to approximately 3.5 Å resolution around the *c** axis, diffraction spots around the *a** axis exhibited only 6 Å resolution. The severe anisotropy of the crystal suggested that the TAF-I$\beta\Delta$C molecules were disordered in the crystal lattice. The preliminary analysis with cryoprotectants suggested that improvement of crystal quality using only cryocondition optimization would be difficult. Thus, we tried to utilize variant proteins to substantially improve the crystal quality of TAF-I$\beta\Delta$C.

### 3.2. Strategy for amino-acid substitutions for crystal-quality improvement

The amino-acid residues to be substituted were selected to meet the following requirements. Firstly, since we wanted to avoid a time-consuming process to find new crystallization conditions for each variant protein, we used an amino-acid substitution that was unlikely to change the crystallization conditions. Since the substitution of surface amino-acid residues of the target protein can change the original crystal form by changes in the epitope(s) for inter-protein contacts in the crystal (Mateja *et al.*, 2002; Longenecker *et al.*, 2001; McElroy *et al.*, 1992), we decided to substitute buried hydrophobic residues.

Secondly, the effect of the amino-acid substitution needed to be small in order to avoid a global structural change, which would presumably cause loss of function of the protein. Since the amino-acid replacements that frequently occur in evolution are unlikely to destroy the protein structure, the replacement pairs should be Leu–Ile, Leu–Met, Ile–Met, Val–Met, Val–Ile and so on (Schulz & Schirmer, 1978). It should be noted that the relatively small effects of these substitutions seem to allow the accumulation of the effects of several amino-acid substitutions. The concept of the physical perturbation method (Kidokoro, 1998) suggests that the effects of the amino-acid substitutions are additive when the effect of each substitution is small.

### 3.3. Crystal-quality improvement with a variant protein and post-crystallization treatment

Since there are only two methionines in TAF-I$\beta\Delta$C, at the N- and C-termini, the replacement of Leu with Met was chosen in the present study in order to utilize the introduced Met residues for MAD phasing. The effects of the amino-acid substitution of Leu/Ile to Met on protein structure have been intensively studied using T4 lysozyme and hen egg-white lysozyme (Gassner *et al.*, 1996; Ohmura *et al.*, 2001) and suggest that proteins are tolerant to this substitution. Therefore, the replacement of Leu with Met seemed to be suitable for the present purpose.

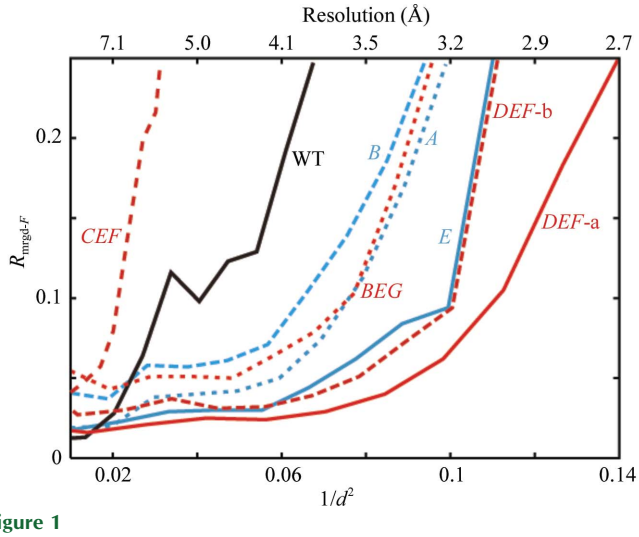


**Figure 1**
Improvement of the TAF-I$\beta\Delta$C crystal by amino-acid substitution(s) and cryo-handling. $R_{\rm mrgd\text{-}\mathit{F}}$ values of the best data from each variant are plotted against resolution [$(1/d)^2$]. *DEF*-a and *DEF*-b represent data from the crystals of variant *DEF* with and without optimization of the soaking conditions, respectively. These values were calculated using *TRUNCATE* in the *CCP*4 program suite (Collaborative Computational Project, Number 4, 1994).

Initially, three TAF-I$\beta\Delta$C variants with single amino-acid substitutions, variants *A* (Leu45Met), *B* (Leu54Met) and *E* (Leu145Met), were prepared and crystallized. The three Leu residues that were replaced with methionine were randomly selected from the 15 Leu residues in TAF-I$\beta\Delta$C. The diffraction data of the three variants were collected at 95 K with cryoprotection and crystal annealing (Table 1). However, the variant proteins only showed marginal improvement in diffraction quality compared with the wild type. Crystal soaking in the trehalose solution before cryoprotection was then tried because soaking in polyol solutions had been observed to sometimes improve the diffraction quality of crystals (Sousa, 1995). Artificial mother liquor containing 30%(*w*/*v*) trehalose was added to a sitting drop at a 1:1 volume ratio and the sitting drop was stored overnight at 293 K. The final concentration of trehalose was therefore 15%(*w*/*v*) in the soaking solution. After the soaking, the crystal was cryoprotected and flash-cooled. Of the three variant crystals, the diffraction data from variant *E* crystals showed the best improvement in isotropy and resolution (Table 1, Fig. 1 and Supplementary Fig. 1*c*). The best crystal of variant *E* diffracted X-rays to 2.75 Å resolution around the *c** axis. However, many diffraction spots still exhibited streaky shapes and the Wilson plot showed a high overall *B* factor (66.4 Å$^2$). In addition, the diffraction data still showed severe anisotropy (see the $\Delta B$ column of Table 1).

Since none of the five MAD data sets from variant *E* crystals were able to provide proper phases for structure determination, another three TAF-I$\beta\Delta$C variants with triple amino-acid substitutions, each of which included the amino-acid substitution at site *E*, were prepared (Supplementary Fig. 2). Of the three TAF-I$\beta\Delta$C variants [variants *DEF* (Leu104Met, Leu145Met, Leu166Met), *BEG* (Leu54Met, Leu145Met, Leu204Met) and *CEF* (Leu74Met, Leu145Met, Leu166Met)], the crystals of variant *DEF* showed a significant reduction in diffraction anisotropy with the same overnight soaking and cryoprotection as used for the variant *E* crystals, while the *BEG* and *CEF* variant crystals showed no improvement of their anisotropic character (Table 1, Fig. 1 and Supplementary Fig. 3). In addition, the number of streaky spots was significantly reduced in the diffraction pattern of the variant *DEF* crystal when compared with that of the variant *E* crystals. It is of note that the space group of the variant *DEF* crystals changed from *C*2 to $P2_1$ when the crystal was flash-cooled after soaking in the trehalose solution (Table 1). However, the space group of the variant *DEF* crystals did not change at room temperature (without flash-cooling) even after soaking in the trehalose solution (Table 2), suggesting that the space-group change occurred during flash-cooling. The space group of the crystals soaked in the glucose solution did not change upon flash-cooling and the resolution did not improve (Tables 1 and 2). Therefore, trehalose seems to play a specific role in improving the crystal quality of TAF-I$\beta\Delta$C. In fact, it was found that two trehalose molecules bind to one TAF-I$\beta\Delta$C dimer in the crystal (Fig. 2).

Despite the improvement in the crystal quality, crystals of variant *DEF* that were soaked overnight with trehalose at 293 K still showed slight anisotropy (see the $\Delta B$ column of Table 1). Optimization of the soaking conditions was therefore performed through adjustment of the soaking time and temperature. The anisotropic character of the diffraction data was improved when the crystals of variant *DEF* were soaked in the trehalose solution at 277 K for 6 h before cryoprotection and flash-cooling (Table 1, Supplementary Fig. 2). Crystal annealing did not improve the crystal quality in this case. It should be noted that cocrystallization with trehalose [variant *DEF*(cocrystal)] did not lead to the substantial crystal-quality improvement that was observed in the variant *DEF* crystals soaked in the trehalose solution [variant *DEF*(soaking)], even though the TAF-I$\beta\Delta$C molecules in the crystal of variant *DEF*(cocrystal) bind trehalose at the same positions as the crystal of variant *DEF*(soaking) (Supplementary Fig. 4).

The diffraction data for MAD phasing were collected using the crystal of variant *DEF*(soaking) and allowed crystal structure deter-

**Table 2**
Unit-cell parameters of the TAF-I$\beta\Delta$C crystals.

Means and standard deviations are given when multiple data were collected.

| Variant/soaking solution† | *a* (Å) | *b* (Å) | *c* (Å) | $\beta$ (°) | Space group |
|---|---|---|---|---|---|
| Wild/30% trehalose (1) | 133.3 | 62.6 | 61.6 | 91.2 | *C*2 |
| *A*/30% trehalose (4) | 125.2 ± 2.3 | 61.7 ± 0.6 | 61.0 ± 0.1 | 91.3 ± 0.1 | *C*2 |
| *B*/30% trehalose (1) | 129.9 | 63.0 | 61.5 | 92.4 | *C*2 |
| *E*/30% trehalose (5) | 123.7 ± 2.4 | 63.2 ± 0.2 | 61.0 ± 0.1 | 90.5 ± 0.5 | *C*2 |
| *DEF*‡/30% trehalose (8) | 61.0 ± 0.2 | 64.3 ± 0.2 | 124.0 ± 0.8 | 90.8 ± 0.2 | $P2_1$ |
| *DEF*§/30% trehalose (7) | 61.0 ± 0.1 | 64.0 ± 0.1 | 123.5 ± 0.7 | 90.3 ± 0.7 | $P2_1$ |
| *BEG*/30% trehalose (3) | 123.7 ± 1.7 | 61.7 ± 0.7 | 61.4 ± 0.0 | 92.1 ± 0.1 | *C*2 |
| *CEF*/30% trehalose (1) | 122.8 | 63.6 | 60.9 | 89.1 | *C*2 |
| *DEF*/30% glucose (1) | 128.7 | 60.7 | 61.6 | 93.1 | *C*2 |
| *DEF* (without soaking) (1) | 134.8 | 60.2 | 61.5 | 94.9 | *C*2 |
| *DEF*/trehalose (1) (cocrystal) | 117.2 | 63.6 | 61.2 | 90.2 | *C*2 |
| *DEF*¶/30% trehalose (3) | 140.4 ± 3.8 | 65.1 ± 0.2 | 61.6 ± 0.1 | 93.8 ± 0.8 | *C*2 |

† Numbers in parentheses show the number of crystals used in preparing the table. ‡ Crystals soaked in the trehalose solution at 293 K. § Crystals soaked in the trehalose solution at 277 K. ¶ No complete data sets were collected owing to decay of the crystals on X-ray irradiation. Diffraction data were collected at room temperature.

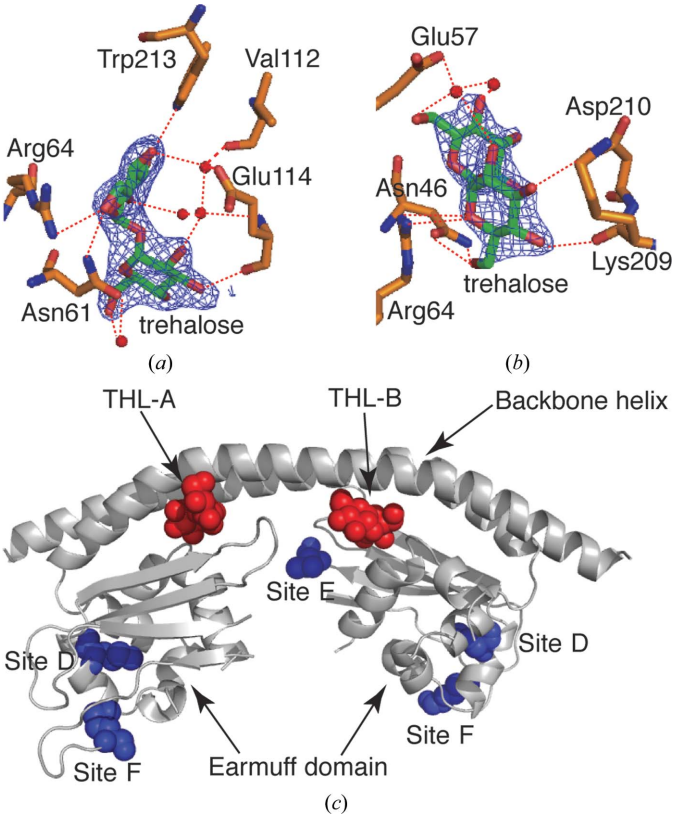


**Figure 2**
Trehalose-binding geometry and sites of amino-acid substitutions. (*a*, *b*) The hydrogen-bond network around the bound trehalose at (*a*) binding site *A* (THL-*A*) and (*b*) binding site *B* (THL-*B*). Simulated-annealing OMIT maps for the bound trehaloses are also shown. The maps are contoured at the 3.5$\sigma$ level. (*c*) The positions of bound trehalose at binding sites *A* and *B* (red) and of the introduced methionine residues, sites *D*, *E* and *F* (blue), are shown in the dimeric TAF-I$\beta\Delta$C molecule.

mination by the MAD method at 2.3 Å resolution (Muto *et al.*, 2007). Higher resolution diffraction data with $R_{\rm mrgd\text{-}F}$ values larger than 0.25 were incorporated in the MAD phasing and crystallographic refinement. The $R_{\rm mrgd\text{-}F}$ values of the diffraction data used in the crystallographic refinement were 0.118 and 0.359 for all reflections (15.0–2.30 Å) and the outer shell reflections (2.42–2.30 Å), respectively.

### 3.4. Analysis of the effects of trehalose and amino-acid substitutions

The crystal structure obtained revealed the positions of the substituted amino acids and bound trehalose in the TAF-I$\beta$ structure. Trehalose molecules were located between the backbone helix and the earmuff domain of each subunit of the dimeric TAF-I$\beta$ molecule. Each trehalose molecule forms nine hydrogen bonds to the protein molecule (Figs. 2*a* and 2*b*). Amino-acid substitution sites *D* (Leu104Met), *E* (Leu145Met) and *F* (Leu166Met) are located in the earmuff domain of TAF-I$\beta\Delta$C (Muto *et al.*, 2007; Fig. 2*c*). There are no interactions between these introduced Met residues. The introduced Met residues at sites *D* and *F* are mostly buried in the molecule. On the other hand, the Met residue at site *E* is located in the loop region and is exposed to solvent. However, the Met residue of site *E* was confirmed not to be involved in intermolecular interactions or a hydrogen-bond network. No interactions were found between bound trehalose and these introduced Met residues.

## 4. Discussion

In the present study, the crystal quality of TAF-I$\beta\Delta$C was significantly improved by amino-acid substitutions and optimization of the soaking conditions. Since it is impossible to screen all protein variants and all conditions for soaking, a strategy to find crystals suitable for structure determination is important. In the present study, the appropriate variant proteins were initially screened without intensive optimization of the crystallization and soaking conditions. After obtaining a variant protein crystal that showed reasonable diffraction-quality improvement, intensive optimization of the soaking conditions was performed (Supplementary Fig. 2). The optimization of the crystallization conditions of variant *DEF* (cocrystal) was therefore not performed in the present study. Another type of strategy can of course be considered: it would be possible to intensively optimize the crystallization conditions of each variant protein. However, we did not utilize this strategy because the optimization of the crystallization conditions for each variant would be a time-consuming process. Therefore, the optimization of the crystallization conditions in the present study was limited.

Another important point in the present study involves the criteria used to assess the crystal quality. In order to select appropriate diffraction data for structure determination, the resolution–$R_{\rm mrgd\text{-}F}$ (or $R_{\rm merge}$) value plot (Diederichs & Karplus, 1997) and visual inspection of diffraction patterns were frequently utilized because these data can be obtained in the typical data-processing procedure and their analysis is relatively easy. In the present study, we used the following methods. Firstly, the quality of the diffraction was assessed by visual inspection of the diffraction spots (Supplementary Figs. 1 and 3). After data processing and scaling, the data sets were compared with regard to the anisotropy of the diffraction data and the overall *B* factors (Table 1), as well as the resolution–$R_{\rm mrgd\text{-}F}$ plot of the crystal (Fig. 1). Assessment of the anisotropy is important in the present study because the significant anisotropy of the diffraction data hampered crystal structure determination. The reflection mosaicity is another well known indicator of macromolecular crystal perfection and detailed analyses of the reflection mosaicity have been reported to evaluate crystal quality (Bellamy *et al.*, 2000; Borgstahl *et al.*, 2001). However, a precise evaluation of the mosaicity could not be preformed in the present study because a specific experiment and calculation are required (Bellamy *et al.*, 2000). The mosaicity shown in Table 1 was provided as a result of analysis of the reflection data using the program *XDS* and was not utilized to assess the diffraction quality.

By utilizing the strategy and criteria described above, we could significantly improve the crystal quality of TAF-I$\beta\Delta$C. Firstly, we chose trehalose as the best reagent for cryoprotection (see §3.1). Amino-acid substitutions and soaking conditions were then examined. As a result, the best diffraction data set (in the present study), which was used in the crystallographic refinement at 2.3 Å resolution, was obtained from a crystal of variant *DEF*. The crystal was soaked in the trehalose solution at 277 K for 6 h before cryoprotection and flash-cooling (Table 1, Supplementary Fig. 2). Although soaking with glucose was also tested, the crystal quality was not significantly improved (Table 1). In addition, soaking in glycerol solution was unlikely to improve the crystal quality because crystals gradually dissolved in artificial mother liquor containing 30%(*v*/*v*) glycerol. It should be noted that cryoprotection with trehalose was essential for the collection of high-quality diffraction data; ice rings frequently appeared without cryoprotection.

Next, the mechanism of the crystal-quality improvement is discussed on the basis of the crystal structure of TAF-I$\beta\Delta$C. Since none of the introduced methionine residues were involved in intermolecular interactions in the crystal or the hydrogen-bond network (Fig. 2*c*), small structural and dynamical perturbations of the TAF-I$\beta\Delta$C variant structure caused by amino-acid substitutions seem to affect the crystal quality. However, the critical event for crystal-quality improvement seemed to be the space-group transition from $C2$ to $P2_1$ of the variant *DEF* crystals soaked in the trehalose solution (Table 1, Supplementary Fig. 5). Small shifts of the molecules, typically about 4–5 Å, during flash-cooling are likely to improve the crystal packing of the variant *DEF* crystals. This type of space-group change has also been reported previously, in which crystals soaked in glycerol solution showed a space-group transition upon flash-cooling (Skrzypczak-Jankun *et al.*, 1996). In the present study, the trehalose functions not only as a cryoprotectant but also as a stabilizing agent for TAF-I$\beta\Delta$C. The intensive hydrogen bonds around the bound trehaloses (Figs. 2*a* and 2*b*) connect the backbone helix and earmuff domain and seem to stabilize the orientation of the earmuff domain, leading to a reduction of the dynamic disorder of TAF-I$\beta\Delta$C in the crystal. This stabilization in the crystal seems to facilitate the re-orientation of TAF-I$\beta\Delta$C molecules in the crystal upon flash-cooling. The other cryoprotectants tested in the present study, glycerol and glucose, were unlikely to bind to the same site with intensive hydrogen bonds. These reagents did not seem to stabilize the orientation of the earmuff domain. Indeed, glucose and glycerol showed no significant cryoprotectant effect.

Since the cocrystallization of variant *DEF* with trehalose resulted in almost identical trehalose binding to TAF-I$\beta\Delta$C (Supplementary Fig. 4), the TAF-I$\beta\Delta$C in the cocrystallized crystals also seemed to be stabilized. However, crystallization with the stabilized TAF-I$\beta\Delta$C (Sousa, 1995) seemed to lead to a significantly smaller unit-cell parameter (*a* axis) in the cocrystallized crystal (Table 2); the stabilized orientation of the earmuff domain may affect the formation of the crystal lattice. The crystal obtained by cocrystallization did not show the crystal lattice transition during flash-cooling (Table 1), probably because its small unit cell inhibits molecular re-orientation in the crystal. As a result, the cocrystallized crystal showed only limited crystal-quality improvement.

Binding of trehalose seems to be effective for crystal-quality improvement of TAF-I$\beta\Delta$C when it occurs in the crystal lattice (or occurs after crystallization). Treatments of crystals (or proteins) should be applied in a specific order, because one treatment of the crystal (or protein) seems to affect the results of subsequent treatments. Further systematic study of the amino-acid substitutions of hydrophobic residues in combination with cryocondition optimization should offer a new strategy for crystal engineering.

We would like to thank Y. Akai for helping with the biochemical analysis. This study was supported in part by the New Energy and Industrial Technology Development Organization (NEDO) of Japan, the Exploratory Research for Advanced Technology Organization (ERATO) of Japan's Science and Technology Agency (JST) and the Ministry of Education, Culture, Sports, Science and Technology of Japan.

## References

Bellamy, H. D., Snell, E. H., Lovelace, J., Pokross, M. & Borgstahl, G. E. O. (2000). *Acta Cryst.* D**56**, 986–995.
Borgstahl, G. E. O., Vahedi-Faridi, A., Lovelace, J., Bellamy, H. D. & Snell, E. H. (2001). *Acta Cryst.* D**57**, 1204–1207.
Chait, B. T. (1994). *Structure*, **2**, 465–467.
Collaborative Computational Project, Number 4 (1994). *Acta Cryst.* D**50**, 760–763.
Cooper, D. R., Boczek, T., Grelewska, K., Pinkowska, M., Sikorska, M., Zawadzki, M. & Derewenda, Z. (2007). *Acta Cryst.* D**63**, 636–645.
Derewenda, Z. S. & Vekilov, P. G. (2006). *Acta Cryst.* D**62**, 116–124.
Diederichs, K. & Karplus, P. A. (1997). *Nature Struct. Biol.* **4**, 269–275.
Gassner, N. C., Baase, W. A. & Matthews, B. W. (1996). *Proc. Natl Acad. Sci. USA*, **93**, 12155–12158.
Jenkins, T. M., Hickman, A. B., Dyda, F., Ghirlando, R., Davies, D. R. & Craigie, R. (1995). *Proc. Natl Acad. Sci. USA*, **92**, 6057–6061.
Kabsch, W. (1993). *J. Appl. Cryst.* **26**, 795–800.
Kidokoro, S. (1998). *Adv. Biophys.* **35**, 121–143.
Lawson, D. M., Artymiuk, P. J., Yewdall, S. J., Smith, J. M., Livingstone, J. C., Treffry, A., Luzzago, A., Levi, S., Arosio, P., Casareni, G., Thomas, C. D., Shaw, W. V. & Harrison, P. M. (1991). *Nature (London)*, **349**, 541–544.
Longenecker, K. L., Garrard, S. M., Sheffield, P. J. & Derewenda, Z. S. (2001). *Acta Cryst.* D**57**, 679–688.
Mateja, A., Devedjiev, Y., Krowarsch, D., Longenecker, K., Dauter, Z., Otlewski, J. & Derewenda, Z. S. (2002). *Acta Cryst.* D**58**, 1983–1991.
McElroy, H. E., Sisson, G. W., Schoettlin, W. E., Aust, R. M. & Villafranca, J. E. (1992). *J. Cryst. Growth*, **122**, 265–272.
Muto, S., Senda, M., Adachi, N., Suzuki, T., Nagai, R., Senda, T. & Horikoshi, M. (2004). *Acta Cryst.* D**60**, 712–714.
Muto, S., Senda, M., Akai, Y., Sato, L., Suzuki, T., Nagai, R., Senda, T. & Horikoshi, M. (2007). *Proc. Natl Acad. Sci. USA*, **104**, 4285–4290.
Ohmura, T., Ueda, T., Hashimoto, Y. & Imoto, T. (2001). *Protein Eng.* **14**, 421–425.
Pflugrath, J. W. (1999). *Acta Cryst.* D**55**, 1718–1725.
Schlatter, D., Thoma, R., Küng, E., Stihle, M., Müller, F., Borroni, E., Cesura, A. & Hennig, M. (2005). *Acta Cryst.* D**61**, 513–519.
Schulz, G. E. & Schirmer, R. H. (1978). *Principles of Protein Structure.* Berlin: Springer–Verlag.
Skrzypczak-Jankun, E., Bianchet, M. A., Amzel, L. M. & Funk, M. O. (1996). *Acta Cryst.* D**52**, 959–965.
Sousa, R. (1995). *Acta Cryst.* D**51**, 271–277.
Strong, M., Sawaya, M. R., Wang, S., Phillips, M., Cascio, D. & Eisenberg, D. (2006). *Proc. Natl Acad. Sci. USA*, **103**, 8060–8065.
Zhou, X. E., Wang, Y., Reuter, M., Mackeldanz, P., Krüger, D. H., Meehan, E. J. & Chen, L. (2003). *Acta Cryst.* D**59**, 910–912.